Desalination and Water Treatment
www.deswater.com
doi: 10.1080/19443994.2013.763387

51 (2013) 6091–6100
September

Taylor & Francis
Taylor & Francis Group

Kinetic, thermodynamic, and equilibrium studies for adsorption of azo reactive dye onto a novel waste adsorbent: charcoal ash

İsmail Özbay*, Utkan Özdemir, Bilge Özbay, Sevil Veli

Department of Environmental Engineering, University of Kocaeli, İzmit 41380, Turkey
Tel. +90 262 3033202; Fax: +90 262 3033005; email: iozbay@kocaeli.edu.tr

Received 28 October 2012; Accepted 31 December 2012

ABSTRACT

This paper investigates the usability of activated charcoal ash for removal of reactive azo dye from aqueous solution. Firstly, elemental composition and surface characteristics of the ash have been examined by using X-ray fluorescence and scanning electron microscopy. The effects of pH, ash dosage, initial dye concentration, agitation period, agitation speed, and temperature were determined by batch experiments. Calculated thermodynamic parameters indicated exothermic and spontaneous characteristics of the adsorption process. Langmuir, Freundlich, and Temkin adsorption isotherms were applied to examine the efficiency of charcoal ash. The obtained correlation coefficients and the considered isotherm parameters showed fitness of the applied isotherm models. Pseudo-second-order kinetic model was found to best represent the kinetic data considering closer values of experimental and calculated dye amounts adsorbed by unit ash mass. Results of the study demonstrated usability of activated charcoal as a promising adsorbent in dye adsorption.

Keywords: Charcoal ash; Azo dye; Thermodynamic analysis; Adsorption isotherms; Reaction kinetics

1. Introduction

Color is one the major indicators of water pollution that reduces photosynthetic activity by preventing proper sunlight penetration [1]. Wastewater effluents containing different synthetic dyes are the main source of color problem in aquatic ecosystems. As these synthetic dyes are widely used in many industrial branches such as dye manufacturing, textile finishing, food coloring, cosmetics, paper industries, etc. enormous volumes of colored wastewaters have been discharged to aqueous media all over the world. Stable and recalcitrant nature of the dyes complicates biological degradation in the discharged media. Furthermore, their toxic and potentially carcinogenic characteristics may cause serious irreversible damages in living organisms [2,3].

As chemical structures of the synthetic dyes exhibit remarkable diversities, several ways have been improved for their classification. The main structure of all synthetic dyes has been composed of two major groups: chromophore and auxochrome. Chromophore compounds control the color of the dyes whereas auxochrome groups alter both wavelength and intensity of adsorption [4]. Based on chromophores, numerous dye groups can arise such as azo, anthraquinone, phthalocyanine, triarylmethane, etc. If their solubility characteristics are considered, acid, mordant, metal complex, direct, basic, and reactive dyes are classified

---

*Corresponding author.

as soluble whereas azoic, sulfur, vat, and disperse dyes are included in insoluble dye class. Dyes can also be classified on basis of their electrical charge as anionic (direct, acid, and reactive dyes), cationic (basic dyes), and nonionic (disperse dyes) [5].

Among these types, azo reactive dyes constitute a major group. They are widely used especially in textile sector all over the world [6]. Azo dyes are highly water soluble due to presence of $-SO_3^-$, $-COO^-$, and OH^- groups. Their recalcitrant nature can be attributed to nitrogen–nitrogen double bonds and sulfonate groups in the structure [7]. They exhibit low biodegradability and they are assumed to be more problematic compared to other forms as their precursors and degradation products are highly carcinogenic [8].

Efficient removal of azo reactive dyes from wastewaters becomes obligatory considering the mentioned harmful impacts. There are various methods used for treatment colored waste waters such as coagulation, ion exchange, adsorption, ultra filtration, ozonation, and reverse osmosis. Among these methods adsorption is regarded to be superior due to several important advantages such as simplicity of design, ease of operation, and insensitivity to toxic materials [9]. Operational costs may also be decreased remarkably by using alternative low-cost adsorbents such as rice husk [10], treated cotton [11], hazelnut shell [12], fruit peels [13], wood sawdust [12], sunflower stalk [14], zeolites [15] pumice [16], durian peel [17], and sugar beet pulp [18].

In this work, we have aimed to investigate usability of charcoal ash for adsorption of azo reactive dye from aqueous solutions. Charcoal ash has been preferred as it is an easily available waste material especially coming from barbecues and restaurants in Turkey. With this aim, first we have analyzed the effects of pH, ash dosage, dye concentration, agitation period, agitation speed, and temperature on adsorption efficiency. In order to determine the impacts of temperature in detail thermodynamic analyses were performed. Langmuir, Freundlich, and Temkin isotherm models were applied to experimental data and isotherm constants were calculated. Furthermore, pseudo-first- and pseudo-second-order kinetic models were used to determine adsorption mechanism and adsorption characteristic constants.

2. Materials and method

2.1. Instrumentation and materials

Charcoal ash obtained from barbecue restaurants was used to remove the reactive azo dye (CIBACRON NAVY P-2R-01). CIBACRON NAVY P-2R-01 has been composed of two different sulphonated dyes containing mono and two azo groups. Chemical structure of the dye is shown in Fig. 1.

The charcoal ash has been washed with distilled water three times in order to remove impurities and sieved through 1 mm pore sieve. In order to improve the adsorption capacity of the charcoal ash, a known amount of ash has been treated by 1 N H_2SO_4 solution for 24 h agitation period. The mixture has been filtered and washed five times with distilled water. Filtered ash has been dried at 105°C for 24 h. The activated ash has been stored in the desiccators. Elemental composition of the charcoal ash has been determined by Philips PW-2404 wavelength dispersive XRF spectrometer. Multipoint Brunauer-Emmett-Teller (BET) specific surface area and pore dimension of the adsorbent have been measured by Quantachrome Nova 4000E model surface analyzer. Analysed results have been summarized in Section 3.1. In the study, scanning electron microscopy (SEM) analyses were also performed by JEOL 6,060 type SEM.

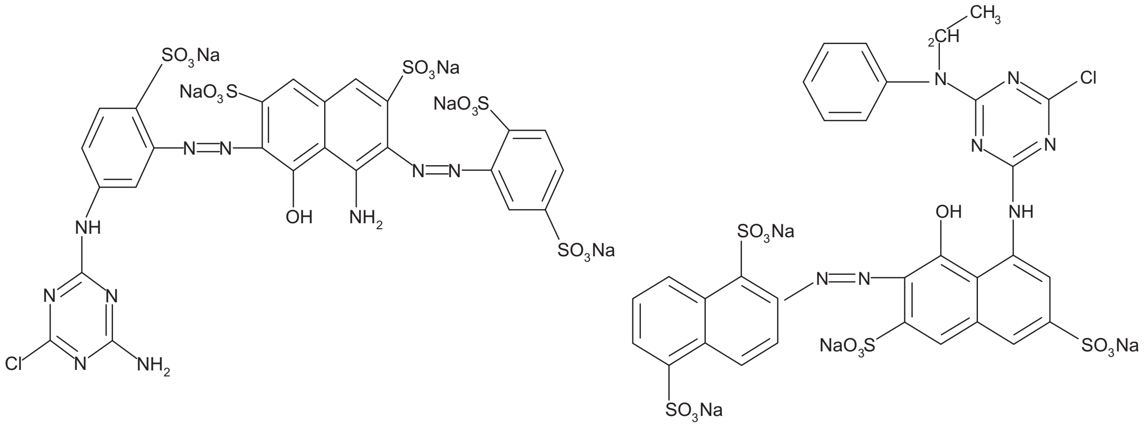

Fig. 1. Chemical structure of the used reactive azo dye.

Batch adsorption tests were carried out by NUVE ST-402 model shaker. Dye concentrations have been determined by using HACH-LANGE DR 2000 model spectrophotometer at 622 nm wavelengths. Thermo Scientific Orion 3-Star Plus pH meter was used for pH adjustments.

2.2. Batch adsorption tests

Batch adsorption technique has been used in the experiments. Samples with different dye concentrations have been prepared by diluting 1,000 mg/L of dye stock solution. The volume of the samples was decided as 50 mL. About 0.1 N HCl and 0.1 N NaOH solutions were used for pH adjustments. Ash dosage has been varied in the range of 0.001–0.1 g.

3. Results and discussion

3.1. Characterization of the charcoal ash

Semi-quantitative elemental analyses were performed in order to investigate the chemical composition of the used adsorbent. Ratios of the compounds are presented in Table 1. As seen from the table, CaO compound constitutes the highest proportion in the structure with ratio of 46.48%. This was followed by SO_3 compounds with 46.22% ratio. Furthermore, the structure contains some elements such as TiO_2, ZnO, and MnO_2 which are well known as superior catalysts of wastewater treatment processes. These compounds are also used in adsorption processes in order to improve the adsorption capacities by providing higher specific surface areas and more effective adsorption sites [19]. Presence of these compounds in the composition of the activated ash may enhance efficient adsorption sites during adsorption process.

Table 1
Chemical composition of activated charcoal ash

Compounds	Ratio (%)
Al_2O_3	0.79
BaO	0.14
CaO	46.48
CuO	0.02
Fe_2O_3	0.53
K_2O	0.36
MgO	1.18
MnO_2	1.07
NiO	0.01
P_2O_5	1.11
PbO	0.01
SO_3	46.22
SiO_2	1.75
SrO	0.11
TiO_2	0.20
ZnO	0.04

BET specific surface area and average pore diameter of the used adsorbent were determined as 7.45 m^2/g and 19.36 nm. These results show physical conformity of the charcoal ash for usage in adsorption process.

3.1.1. SEM analysis of the used adsorbent

SEM analysis is a useful tool for investigation of the surface area and structure morphologies of the materials. In the study, SEM images of the used adsorbent were taken before and after the adsorption in order to examine the appropriateness of the activated charcoal ash visually. Fig. 2(a) and (b) are the SEM images of the adsorbent before and after adsorption, respectively.

As seen from Fig. 2(a), surface of the adsorbent exhibits remarkable irregularity and there are significant pores on the surface. Particular structures with sharp edges and heterogeneous size distribution have been observed. The porous surface has been covered by dye molecules significantly after the adsorption process (Fig. 2(b)).

3.2. Effects of experimental conditions on adsorption efficiency

Impacts of pH, adsorbent dosage, initial dye concentration, agitation period, agitation speed, and temperature have been investigated individually for determination of ideal experimental conditions.

3.2.1. Effect of pH

Removal efficiency has been strongly affected by the pH of the solution in adsorption studies [20]. In this study, impact of pH has been investigated by adjusting pH of the dye solutions from 0.5 to 7. In the conducted experiments, 0.03 g activated ash has been added into 50 mL of 40 mg/L dye solution. Samples have been shaken for 90 min in 200 rpm agitation speed. Obtained results are given in Fig. 3.

As seen from the figure, higher adsorption efficiencies have been performed for pH values lower than 3. At strongly acidic media remarkable electrostatic attraction exists between the positively charged surface of the used adsorbent and anionic dye molecules. Increase in pH values causes improvement in amount of negatively charged sites and this causes decrease in adsorption efficiency [1].

In this study, optimum pH has been determined to be 2 considering sufficient adsorption performances of

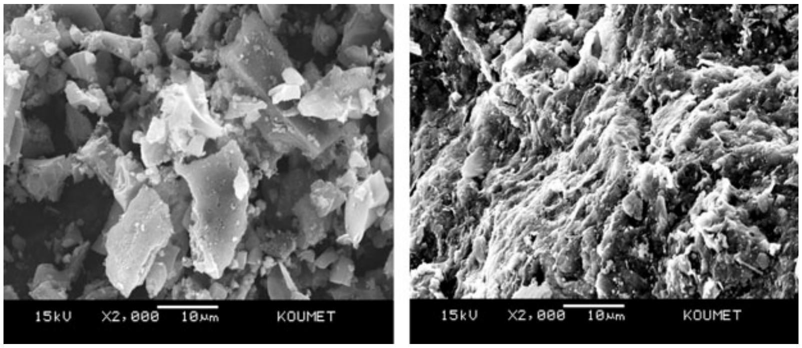

Fig. 2. SEM images of the activated charcoal ash (a) before and (b) after dye adsorption.

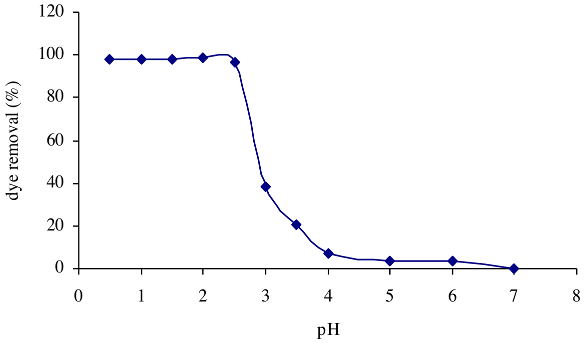

Fig. 3. Effect of pH on adsorption of reactive azo dye by activated charcoal ash (ash dosage 0.03 g/50 mL, initial dye concentration 40 mg/L, contact time 90 min, agitation speed 200 rpm, and temperature 23˚C).

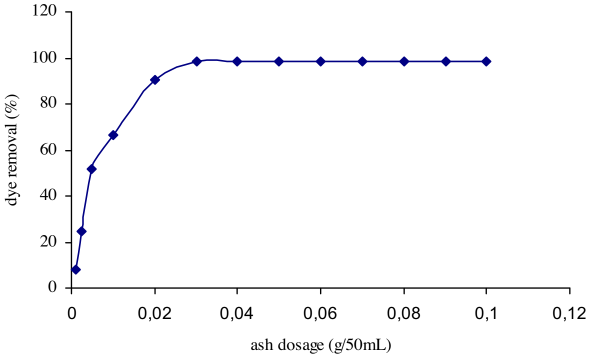

Fig. 4. Effect of adsorbent dosage on adsorption of reactive azo dye by activated charcoal ash (pH 2, initial dye concentration 40 mg/L, contact time 90 min, agitation speed 200 rpm, and temperature 23˚C).

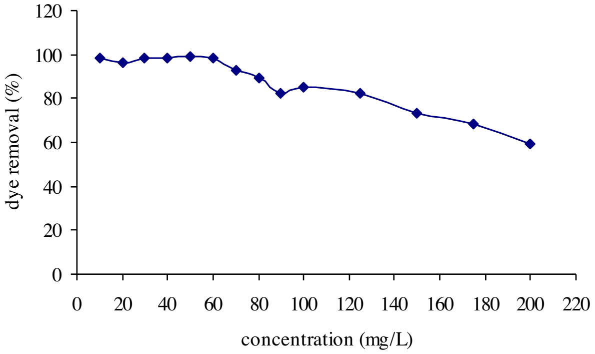

Fig. 5. Effect of initial dye concentration on adsorption of reactive azo dye by activated charcoal ash (pH 2, ash dosage 0.04 g/50 mL, contact time 90 min, agitation speed 200 rpm, and temperature 23˚C).

98%. All forthcoming experimental studies have been performed by adjusting pH to 2.

3.2.2. *Effect of adsorbent dosage*

In order to provide quantitative adsorbate uptake determination of ideal adsorbent dosage is demanded. Commonly increasing adsorbent dosages improve adsorption efficiencies. This can be explained by the increase of surface area where the adsorption takes place [21].

In this study, optimum ash dosage has been determined by using various adsorbent amounts in the range of 0.001–0.1 g. Fig. 4 demonstrates the results clearly.

Optimum ash concentration has been determined to be 0.04 g as the adsorption process reached equilibrium with this dosage and remained stable by increasing amounts.

3.2.3. *Effect of initial dye concentration*

Impacts of initial dye concentration have been examined by using different dye concentrations from 10 to 200 mg/L. As seen from Fig. 5, increasing dye concentrations caused remarkable decrease in adsorption efficiency at concentrations higher than 60 mg/L. Considering the obtained experimental results, ideal dye concentration has been decided to be 50 mg/L for this study.

3.2.4. Effect of agitation period

The agitation period has been regarded as one of the most important factors affecting efficiency of adsorption processes. So, impact of time has been investigated in the study by applying predetermined optimum values of pH, ash dosage, and dye concentration. Obtained results are shown in Fig. 6.

Removal efficiency has exhibited significant increase continuously until 90 min and remained stable in longer periods. About 90 min has been found to be adequate for this study.

3.2.5. Effect of agitation speed

Impact of agitation speed on adsorption efficiency has also been investigated as it affects solute distribution in the bulk solution and external boundary film formation [22]. In the conducted experiments various agitation speeds, in the range from 50 to 250 rpm, have been tested at predetermined optimum contact time of 90 min. Fig. 7 shows the obtained results.

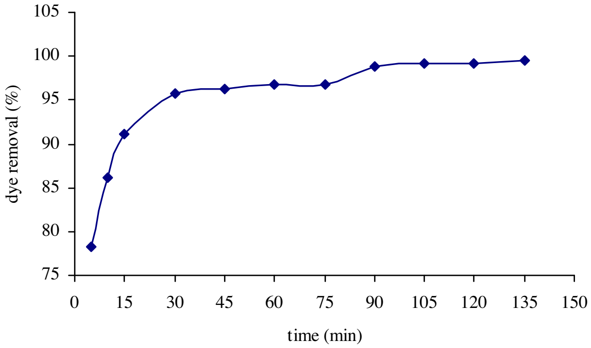

Fig. 6. Effect of agitation period on adsorption of reactive azo dye by activated charcoal ash (pH 2, ash dosage 0.04 g/50 mL, initial dye concentration 50 mg/L, agitation speed 200 rpm, and temperature 23℃).

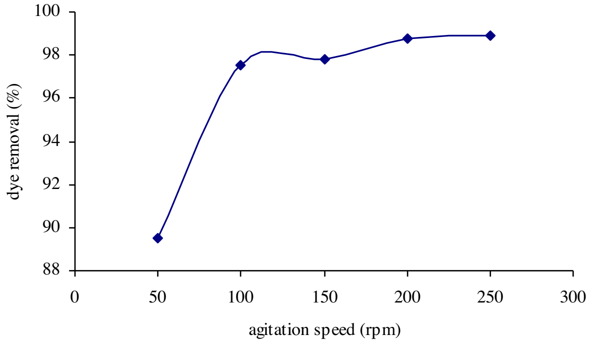

Fig. 7. Effect of agitation speed on adsorption of reactive azo dye by activated charcoal ash (pH 2, ash dosage 0.04 g/50 mL, initial dye concentration 50 mg/L, contact time 90 min, and temperature 23℃).

As seen from the figure agitation speed of 200 rpm will be appropriate for the performed study.

3.2.6. Effect of temperature

Impacts of different temperature conditions (in the range from 20 to 60) have been tested in order to explain the adsorption thermodynamics. Increasing temperature values caused significant decrease in dye adsorption demonstrating exothermic characteristics of the adsorption process (Fig. 8).

Thermodynamic calculations were also performed to investigate the impacts of temperature in detail.

3.3. Thermodynamic analyses

Thermodynamic parameters including free energy change (ΔG), isosteric enthalpy change (ΔH), and entropy change (ΔS) have been calculated in order to evaluate the feasibility of the adsorption process [23]. With this aim following equations were used:

$$K_c = \frac{C_{ads}}{C_e} \tag{1}$$

$$\Delta G = -RT \ln K_c \tag{2}$$

$$\Delta G = \Delta H - T\Delta S \tag{3}$$

$$\ln K_c = \frac{\Delta S}{R} - \frac{\Delta H}{RT} \tag{4}$$

In Eq. (1), K_c represents the equilibrium constant, C_{ads} shows the amount of dye adsorbed on activated at equilibrium (mg/g) and C_e is equilibrium concentration of dye (mg/L). In the following equations, R is

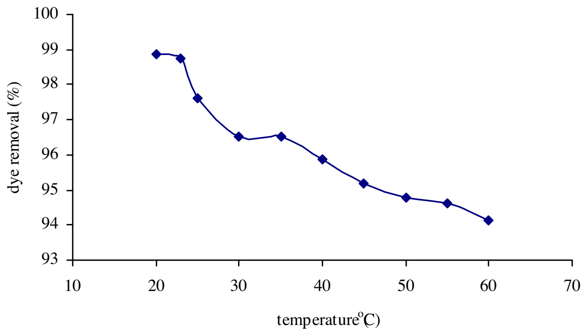

Fig. 8. Effect of temperature on adsorption of reactive azo dye by activated charcoal ash (pH 2, ash dosage 0.04 g/50 mL, initial dye concentration 50 mg/L, contact time 90 min, and agitation speed 200 rpm).

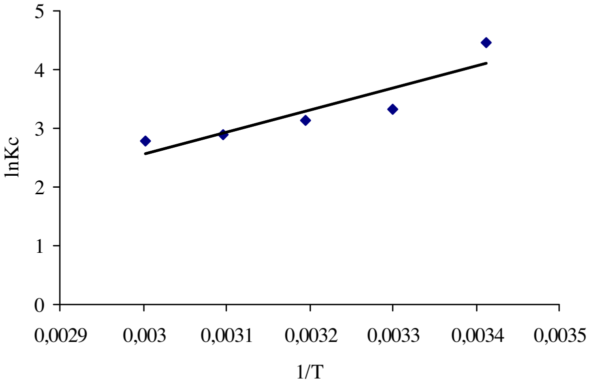

Fig. 9. Van't Hoff plot for the adsorption of dye by activated ash (pH 2, ash dosage 0.04 g/50 mL, initial concentration 50 mg/ L, contact time 90 min., and agitation speed 200 rpm).

Table 2
Thermodynamic parameters for dye adsorption by using activated ash

Temperature (K)	ΔG (kJ/mol)	ΔH^a (kJ/mol)	ΔS^a (J/mol K)
293	−10.87	−31.29	−72.57
303	−8.39		
313	−8.18		
323	−7.80		
333	−7.69		

[a]Measured between 293 and 333 K.

the universal gas constant (J/mol K) and T is absolute temperature (K).

ΔH and ΔS were determined from the slope and intercept of the plot between $\ln K_c$ vs. $1/T$, respectively (Fig. 9).

Calculated ΔG, ΔH, ΔS values are summarized at Table 2. Negative values of ΔG show spontaneous adsorption reactions and negative value of ΔH demonstrates the exothermic characteristic of dye adsorption by activated charcoal ash. Furthermore, physical adsorption process is expected to be dominant as calculated ΔH exists in the range of 10–40 kJ/mol [24]. Negative value of ΔS indicates the regularity of the solute molecules in the adsorption phenomena [20].

3.4. Adsorption isotherm models

In the study Langmuir, Freundlich, and Temkin adsorption isotherm models have been applied in order to examine the amount of dye adsorbed onto the activated charcoal ash as a function of dye concentration at constant temperature.

Adsorption capacity of the used adsorbent was calculated by using following equation:

$$q_e = \frac{(C_0 - C_e)V}{m} \tag{5}$$

In Eq. (5) q_e (mg/g) is the equilibrium adsorption capacity of the ash, C_0 and C_e (mg/L) are the initial and equilibrium concentrations of dye in solution, V (L) is the sample volume, and m (g) is the amount of the ash.

3.4.1. Langmuir isotherm

Langmuir model is a simple theoretical model that assumes monolayer adsorption phenomena containing homogeneous adsorbent surface with identical adsorption sites [25]. Linear equation developed for Langmuir model can be expressed as follow:

$$\frac{C_e}{q_e} = \frac{1}{kV_m} + \frac{C_e}{V_m} \tag{6}$$

where V_m (mg/g) is the monolayer adsorption capacity and k is the empirical equilibrium constant. k and V_m have been determined from the slope and intercept of the Langmuir plot, respectively (Fig. 10).

The essential characteristic of Langmuir isotherm can be expressed by considering dimensionless separation factor (R_L). This parameter can be calculated by using following equation:

$$R_L = \frac{1}{(1 + kC_e)} \tag{7}$$

Calculated R_L values provide information about the type of the adsorption process as [26]:

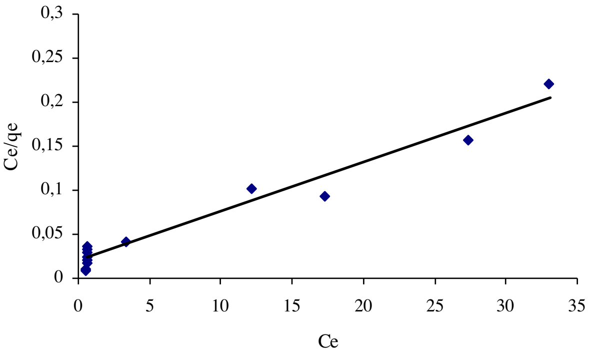

Fig. 10. Langmuir isotherm for the adsorption of dye by activated ash.

Value of R_L	Adsorption type
$R_L > 1.0$	Unfavorable
$R_L = 1.0$	Linear
$0 < R_L < 1.0$	Favorable
$R_L = 0$	Irreversible

R_L value has been determined as 0.85 for this study and this confirms the favorable characteristics of the adsorption.

3.4.2. Freundlich isotherm

The Freundlich isotherm is an empirical equation that is widely applied in adsorption studies to explain heterogeneous systems. Linear form of this model can be written as [27]:

$$\log q_e = \log K_f + \frac{1}{n} \log C_e \tag{8}$$

where K_f is the Freundlich constant that denotes the amount of adsorbate adsorbed for a unit equilibrium concentration and $\frac{1}{n}$ is the adsorption intensity.

In the study, K_f and $\frac{1}{n}$ have been determined from the graph of $\log q_e$ vs. $\log C_e$ (Fig. 11).

In favorable adsorption processes, $\frac{1}{n}$ values change in the range from 0 to 1. In this study, $\frac{1}{n}$ has been calculated as 0.48 confirming suitability of the performed adsorption process.

Value of $\frac{1}{n}$	Adsorption type
$\frac{1}{n} = 1.0$	Linear
$0 < \frac{1}{n} < 1.0$	Favorable
$\frac{1}{n} > 1.0$	Unfavorable

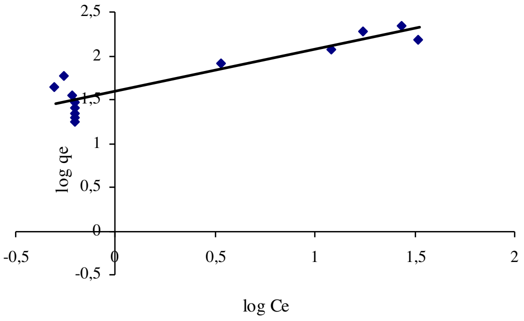

Fig. 11. Freundlich isotherm for the adsorption of dye by activated ash.

3.4.3. Temkin isotherm

Temkin isotherm is another adsorption model considering adsorbate–adsorbate interactions. The model assumes these interactions cause decrease in heat of adsorption of the molecules in the layer and bonding energies exhibit uniform distribution in the adsorption process [28].

This isotherm can be expressed with the following formula:

$$q_e = B \ln A + B \ln C_e \tag{9}$$

In Eq. (9) A denotes Temkin constant used to examine adsorbate–adsorbate interactions and B is the constant related with adsorption heat.

A and B can be determined from plot of q_e vs. $\ln C_e$ (Fig. 12).

All obtained isotherm parameters and r^2 values are summarized in Table 3.

3.5. Adsorption kinetic models

In adsorption studies, kinetic models are applied to experimental data in order to obtain information about the mechanism of adsorption. By this way mass transfer, diffusion control, and chemical reaction mechanisms can be understood better [29]. With this aim, pseudo-first- and pseudo-second-order reaction kinetics are commonly used.

In this study, the initial dye concentrations have been determined as 25, 50, and 75 mg/L for kinetic modeling purposes. The dependences of these concentrations against time are shown in Fig. 13.

3.5.1. Pseudo-first-order model

Pseudo-first-order kinetic model can be applied to explain sorption kinetics [30]. Following equation is developed for this model:

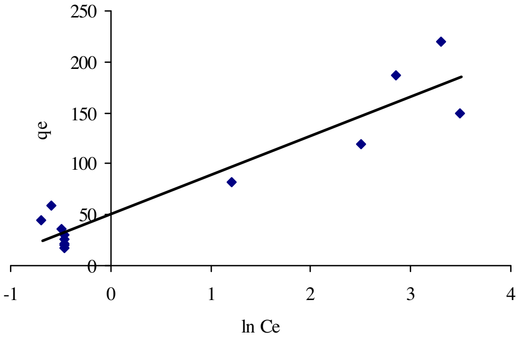

Fig. 12. Temkin isotherm for the adsorption of dye by activated ash.

Table 3
Isotherm parameters determined for adsorption of dye by using activated ash

Langmuir				Freundlich			Temkin		
V_m	k	R_L	r^2	K_f	$1/n$	r^2	A	B	r^2
178.57	0.29	0.85	0.96	38.23	0.48	0.83	3.73	38.28	0.88

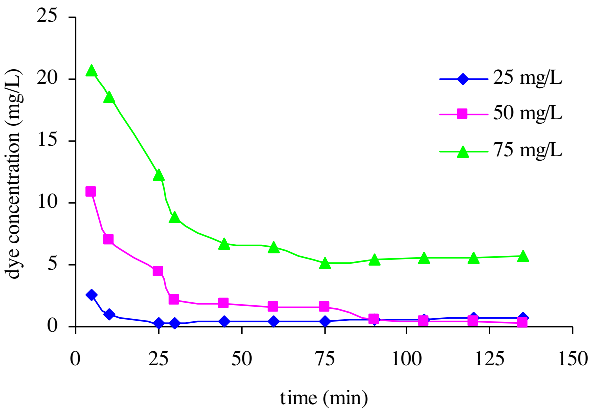

Fig. 13. Kinetics of adsorption of dye on activated ash.

$$\ln(q_e - q_t) = \ln q_e - k_1 t \tag{10}$$

where k_1 represents rate constant of the first order reaction kinetics, q_t and q_e are the amount of dye adsorbed at time t and saturation (mg/g), respectively. k_1 can be determined from the plot of $\ln(q_e - q_t)$ against time (Fig. 14).

As seen from Fig. 14, the plots $\ln(q_e - q_t)$ of vs. t give straight lines for all the tested dye concentrations confirming linearity of Lagergren equation for this study. Furthermore, $q_{e,\text{calculated}}$ values were determined from the intersection points of the curves. Obtained k_1, $q_{e,\text{calculated}}$ and r^2 values are given in Table 4.

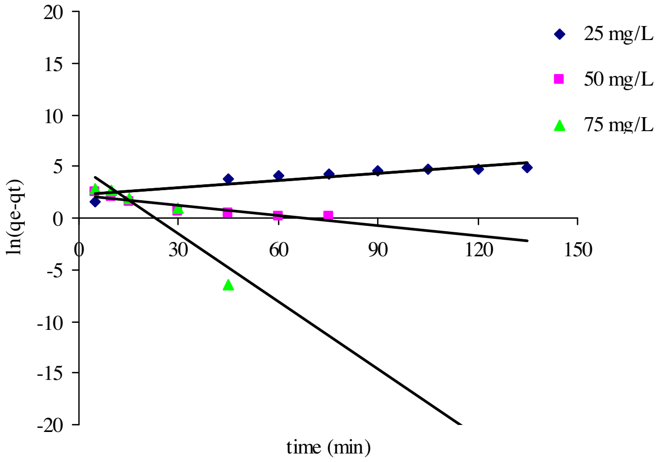

Fig. 14. Pseudo-first-order reaction kinetics for the adsorption of dye on activated ash.

Table 4
Kinetic parameters calculated for dye adsorption on activated ash

Initial dye concentration (mg/L)	$q_{e,\text{experimental}}$ (mg/g)	Pseudo-first-order			Pseudo-second-order		
		k_1 (1/min)	$q_{e,\text{calculated}}$ (mg/g)	r^2	k_2 (g/mg min)	$q_{e,\text{calculated}}$ (mg/g)	r^2
25	30.44	-2.34×10^{-2}	9.11	0.86	1.50×10^{-2}	31.06	0.99
50	61.97	3.30×10^{-2}	9.26	0.84	8.99×10^{-3}	62.89	0.99
75	86.77	21.75×10^{-2}	143.52	0.84	2.49×10^{-3}	90.09	0.99

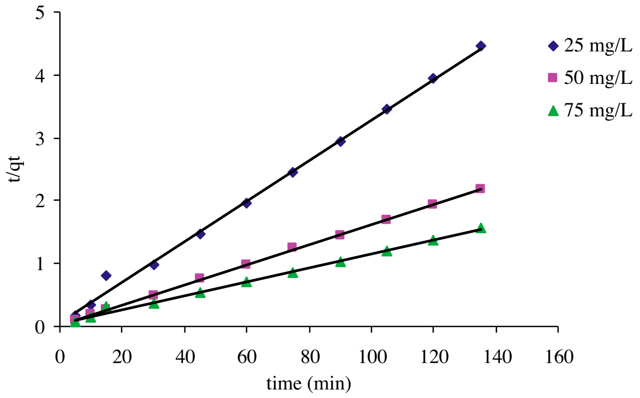

Fig. 15. Pseudo-second-order reaction kinetics for the adsorption of dye on activated ash.

3.5.2. Pseudo-second-order model

The pseudo-second-order kinetic model has been expressed by the following formula [31]:

$$\frac{t}{q_t} = \frac{1}{k_2 q_e^2} + \frac{t}{q_e} \tag{11}$$

In the equation k_2 explains the pseudo-second-order rate constant. Similar to the pseudo-first-order model, k_2 and $q_{\mathrm{e,calculated}}$ can be determined from the plots of $\ln(t/q_t)$ vs. time (Fig. 15).

All calculated kinetic parameters for both pseudo-first and pseudo-second order kinetic models are summarized in Table 4.

Considering closer $q_{\mathrm{e,experimental}}$ and $q_{\mathrm{e,calculated}}$ values and also higher correlation coefficients obtained for pseudo-second-order reaction, it can be concluded that the adsorption mechanism has followed pseudo-second-order reaction kinetics.

Conclusions

In Turkey, ash is among the common components of municipal solid waste compositions. It is continuously produced in barbecue restaurants in remarkable amounts. So it is a cost free and easily available material. Considering these advantages, we have investigated usability of activated charcoal ash for adsorption of reactive azo dye in this manuscript. Chemical composition of ash was analyzed by dispersive XRF spectrometer. Elements such as TiO_2, ZnO, and MnO_2 were found in the structure. Presence of these elements may improve adsorption capacity of the adsorbent. BET specific surface area of $7.45\,m^2/g$ was also found to a promising physical characteristic.

In batch adsorption tests, optimum experimental conditions were examined for the study. Optimum conditions were determined as pH 2, initial dye concentration 50 mg/L, ash dosage 0.04 g/50 mL, agitation period 90 min, agitation speed 200 rpm, and temperature 20°C.

In order to investigate the impacts of temperature on adsorption process, thermodynamic analyses were also performed. Negative ΔG values indicated spontaneous adsorption reactions and ΔH value of -31.29 kJ/mol showed the exothermic characteristic of the process.

Langmuir, Freundlich, and Temkin isotherms were used to evaluate the empirical values. As well as linearity of all models, R_L value of 0.85 and $1/n$ value of 0.48 also confirmed the fitness of isotherm data to Langmuir and Freundlich models, respectively.

Results of the kinetic studies showed that pseudo-second-order reaction kinetic has described the adsorption of azo dye onto activated ash better with closer experimental and calculated values of q_e. Correlation coefficient obtained for pseudo-second-order kinetic model was also higher.

Results of the study demonstrated suitability of activated charcoal ash for removing reactive azo dyes from aqueous solutions. This adsorbent is thought to be a promising alternative for removal of dyes from wastewaters considering its sufficient adsorption efficiency and economical benefits.

Acknowledgment

The authors express their thanks to Serap Gümüş working in Metallurgical and Materials Engineering Department of Kocaeli University for the helpful supports during SEM analyses. This study was funded by the University of Kocaeli Research Fund under Project No. 2012/023.

Nomenclature

A	Temkin constant for adsorbate–adsorbate interactions
B	constant related with adsorption heat
C_{ads}	amount of dye adsorbed on activated at equilibrium
C_e	equilibrium concentration of dye
C_0	initial concentrations of dye
k	empirical equilibrium constant of Langmuir isotherm
k_1	rate constant of the first order reaction kinetics
k_2	pseudo-second-order rate constant
K_c	equilibrium constant for thermodynamic analysis
K_f	the Freundlich constant
m	amount of the ash

$1/n$	adsorption intensity
R	universal gas constant
R_{L}	dimensionless separation factor
r^2	correlation coefficients
t	time
T	absolute temperature
V	sample volume
V_{m}	the monolayer adsorption capacity
q_{e}	the amount of dye adsorbed at saturation
q_t	the amount of dye adsorbed at time t
$q_{\mathrm{e,calculated}}$	calculated value for amount of adsorbed dye per unit ash mass
$q_{\mathrm{e,experimental}}$	experimental value for amount of adsorbed dye per unit ash mass
ΔG	free energy change
ΔH	isosteric enthalpy change
ΔS	entropy change

References

[1] I.D. Mall, V.C. Srivastava, N.K. Agarwal, Removal of orange-G and methyl violet dyes by adsorption onto bagasse fly ash—Kinetic study and equilibrium isotherm analyses, Dyes Pigm. 69 (2006) 210–223.

[2] V.S. Mane, I.D. Mall, V.C. Srivastava, Use of bagasse fly ash as an adsorbent for the removal of brilliant green dye from aqueous solution, Dyes Pigm. 73 (2007) 269–278.

[3] G. Moussavi, M. Mahmoudi, Removal of azo and anthraquinone reactive dyes from industrial wastewaters using MgO nanoparticles, J. Hazard. Mater. 168 (2009) 806–812.

[4] V.K. Gupta, Suhas, Application of low-cost adsorbents for dye removal—A review, J. Environ. Manage. 90 (2009) 2313–2342.

[5] G. Mishra, M. Tripathy, A critical review of the treatments for decolourization of textile effluent, Colourage 40 (1993) 35–38.

[6] Y.H. Lin, J.Y. Leu, Kinetics of reactive azo-dye decolorization by pseudomonas luteola in a biological activated carbon process, Biochem. Eng. J. 39 (2008) 457–467.

[7] E. Forgacs, T. Cserhati, G. Oros, Removal of synthetic dyes from wastewaters: A review, Environ. Int. 30 (2004) 953–971.

[8] M. Neamtu, I. Siminiceanua, A. Yediler, A. Kettrup, Kinetics of decolorization and mineralization of reactive azo dyes in aqueous solution by the UV/H_2O_2 oxidation, Dyes Pigm. 53 (2002) 93–99.

[9] N.K. Amin, Removal of direct blue-106 dye from aqueous solution using new activated carbons developed from pomegranate peel: Adsorption equilibrium and kinetics, J. Hazard. Mater. 165 (2009) 52–62.

[10] M.M. Mohamed, Acid dye removal: comparison of surfactant-modified mesoporous FSM-16 with activated carbon derived from rice husk, J. Colloid. Interf. Sci. 272 (2004) 28–34.

[11] I. Bouzaida, M.B. Rammah, Adsorption of acid dyes on treated cotton in a continuous system, Mater. Sci. Eng. 21 (2002) 151–155.

[12] F. Ferrero, Dye removal by low cost adsorbents: Hazelnut shells in comparison with wood sawdust, J. Hazard. Mater. 142 (2007) 144–152.

[13] G. Annadurai, R.S. Juang, D.J. Lee, Use of cellulose-based wastes for adsorption of dyes from aqueous solutions, J. Hazard. Mater. 92 (2002) 263–274.

[14] G. Sun, X. Xu, Sunflower stalk as adsorbents for color removal from textile wastewater, Ind. Eng. Chem. Res. 36 (1997) 808–812.

[15] V. Meshko, L. Markovska, M. Mincheva, A.E. Rodrigues, Adsorption of basic dyes on granular activated carbon and natural zeolite, Water Res. 35 (2001) 3357–3366.

[16] E.V. Veliev, T. Öztürk, S. Veli, A.G. Fatullayev, Application of diffusion model for adsorption of azo reactive dye on pumice, Pol. J. Environ. Stud. 15 (2006) 347–353.

[17] K. Nuithitikul, S. Srikhun, S. Hirunpraditkoon, Kinetics and equilibrium adsorption of Basic Green 4 dye on activated carbon derived from durian peel: Effects of pyrolysis and post-treatment conditions, J. Taiwan Inst. Chem. E. 41 (2010) 591–598.

[18] V.M. Vučurović, R.N. Razmovski, M.N. Tekić, Methylene blue (cationic dye) adsorption onto sugar beet pulp: Equilibrium isotherm and kinetic studies, J. Taiwan Inst. Chem. E. 43 (2012) 108–111.

[19] Q.U. Jiuhui, Research progress of novel adsorption processes in water purification: A review, J. Environ. Sci. 20 (2008) 1–13.

[20] U. Özdemir, B. Özbay, S. Veli, S. Zor, Modeling adsorption of sodium dodecyl benzene sulfonate (SDBS) onto polyaniline (PANI) by using multi linear regression and artificial neural networks, Chem. Eng. J. 178 (2011) 183–190.

[21] S. Veli, B. Alyüz, Adsorption of copper and zinc from aqueous solutions by using natural clay, J. Hazard. Mater. 149 (2007) 226–233.

[22] G. Crini, H.N. Peindy, F. Gimbert, C. Robert, Removal of C.I. basic green 4 (malachite green) from aqueous solutions by adsorption using cyclodextrin-based adsorbent: Kinetic and equilibrium studies, Sep. Purif. Technol. 53 (2007) 97–110.

[23] N. Gupta, A.K. Kushwaha, M.C. Chattopadhyaya, Adsorption studies of cationic dyes onto Ashoka (*Saraca asoca*) leaf powder, J. Taiwan Inst. Chem. E. 43 (2012) 604–613.

[24] Z.M. Jiang, A.M. Li, J. Cai, C. Wang, Q. Zhang, Adsorption of phenolic compounds from aqueous solutions by aminated hypercrosslinked polymers, J. Environ. Sci. 19 (2007) 135–140.

[25] D. Sun, X. Zhang, Y. Wu, X. Liu, Adsorption of anionic dyes from aqueous solution on fly ash, J. Hazard. Mater. 181 (2010) 335–342.

[26] M. Alkan, M. Doğan, Adsorption of copper (II) onto perlite, J. Colloid Interf. Sci. 243 (2001) 280–291.

[27] B. Alyüz, S. Veli, Kinetics and equilibrium studies for the removal of nickel and zinc from aqueous solutions by ion exchange resins, J. Hazard. Mater. 167 (2009) 482–488.

[28] M.I. Temkin, V. Pyzhev, Kinetic of ammonia synthesis on promoted iron catalyst, Acta. Phys. Sın. 12 (1940) 327–356.

[29] M. Doğan, M. Alkan, Adsorption kinetics of methyl violet onto perlite, Chemosphere 50 (2003) 517–528.

[30] S. Lagergren, About the theory of so-called adsorption of soluble substance, K. Sven. Vetenskapsakad 24 (1898) 1–39.

[31] Y.S. Ho, G. McKay, Kinetic models for the sorption of dye from aqueous solution by wood, Process Saf. Environ. 76 (1998) 183–191.